

Flexible memristors created by 2D printing based on graphene materials

© A.I. Ivanov,¹ R.A. Soots,¹ A.D. Pulik,¹ I.V. Antonova^{1,2}

¹ Rzhanov Institute of Semiconductor Physics, Siberian Branch, Russian Academy of Sciences, 630090 Novosibirsk, Russia

² Novosibirsk State Technical University, 630078 Novosibirsk, Russia
e-mail: art.iv.il@mail.ru

Received March 17, 2024

Revised April 26, 2024

Accepted May 22, 2024 [1mm]

Memristor structures with crossbar architecture were printed on a 2D inkjet printer. To make contacts, a suspension based on graphene particles was used. The memristor active layer was formed based on V_2O_5 nanoparticles encapsulated by fluorinated graphene. Stable resistive switchings were obtained with a ratio of currents in the open and closed states ON/OFF of two orders of magnitude and a switching voltage of 1.0–1.5 V. Currents in the open state increased with increasing area of the structures, which corresponds to conduction through localized states. Tensile strains that occur during bending of more than 2% lead to a decrease in the open state current; these changes are reversible. Varying the structures parameters, and, above all, reducing the active layer thickness makes it possible to switch to a multi-level switching mode. The promise of using such memristors to create non-volatile and multi-level memory with low energy consumption is shown.

Keywords: memristor, crossbar structure, graphene contacts, fluorinated graphene, flexibility, multilevel switchings.

DOI: 10.61011/TP.2024.08.59020.86-24

Introduction

Neuromorphic networks see a sharp increase of scientific interest today [1,2] and the implementation of an artificial network of memristors for computing using neuromorphic processes is one of the most popular areas of development of neuromorphic networks [3–6]. Modern two-dimensional materials such as graphene oxide, fluorinated graphene (FG), MoS_2 and others have demonstrated the prospects for developing thin-film memristors based on them [7–9]. We proposed a method for forming memristor structures using active layers of memristors based on fluorinated graphene [7,10]. The fluorinated graphene is the most stable dielectric compound of graphene, a transparent and flexible material, and due to its ability to encapsulate nanoparticles of another substance, fluorinated graphene-based composites make it possible to create nucleus–shell particles based on fluorinated graphene (FG/ V_2O_5) and use them for production of memristor structures.

The results of implementation of memristor structures made of FG/ V_2O_5 nanoparticles on flexible substrates using 2D-inkjet printing are presented in this study. Memristors were structures with a crossbar architecture and contacts based on graphene flakes. Stable switching, as well as the flexibility of printed memristors and matrices based on them is demonstrated.

1. Preparation of material and creation of structure with a crossbar architecture

The active layer was created using FG and a suspension of vanadium pentoxide nanoparticles with a diameter of ~ 5 – 7 nm. FG was obtained by processing graphene flakes created by chemical stratification of graphite in hydrofluoric acid [11], and vanadium pentoxide was chemically synthesized using the sol-gel method [12]. After the graphene fluorination process, the solution was replaced with water with ethyl alcohol in the proportion of 30:70%, and a suspension containing ~ 2 mg/ml of fluorinated graphene was obtained. The second suspension also contained the same amount of V_2O_5 nanoparticles. Then the suspensions were mixed in a ratio of 1:1. 20% ethylene glycol was added to the suspension to create the ink, and the measured dynamic viscosity of the suspension was about 20 Pa·s. AFM an image of the active layer of the memristor and a schematic image of one element (a nanoparticle from V_2O_5 , encapsulated FG) and the structure of the memristor as a whole are shown in Fig. 1. The studied crossbar structures were created using inkjet printing on a 100 nm thick polyethylene terephthalate substrate on a Dimatix FU-JIFILM DMP-2831 printer with a print resolution of $50 \mu m$, and no spreading of the suspension material was observed for the substrates used. The roughness of the layer of V_2O_5 encapsulated with graphene on a SiO_2/Si substrate is 0.9–1.5 nm on the area of $3 \times 3 \mu m$. Contacts printed from graphene have a roughness of ~ 18 – 22 nm. The

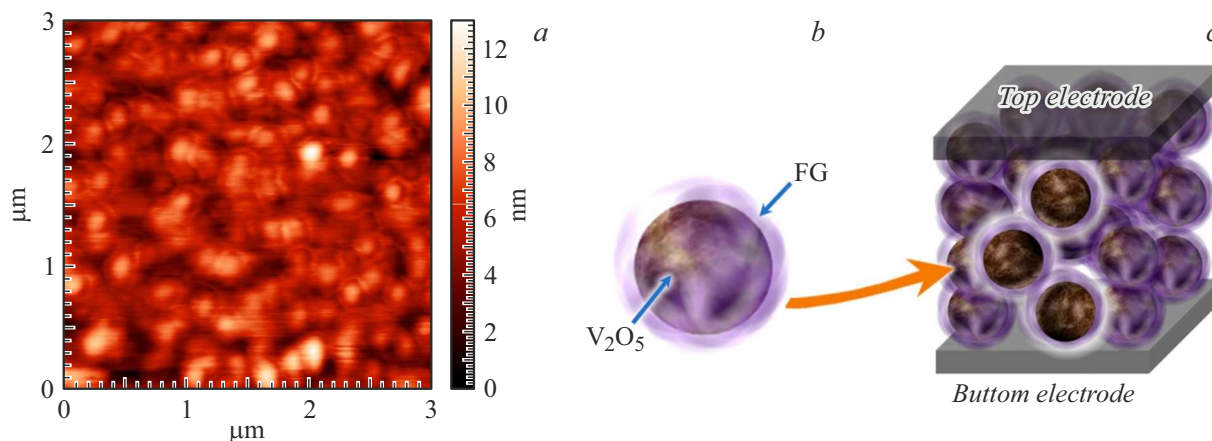


Figure 1. *a* — AFM image of the active memristor layer on graphene contacts and a SiO₂/Si substrate; *b* — schematic image: nanoparticles from V₂O₅ encapsulated with fluorinated graphene; *c* — crossbar of the structure as a whole.

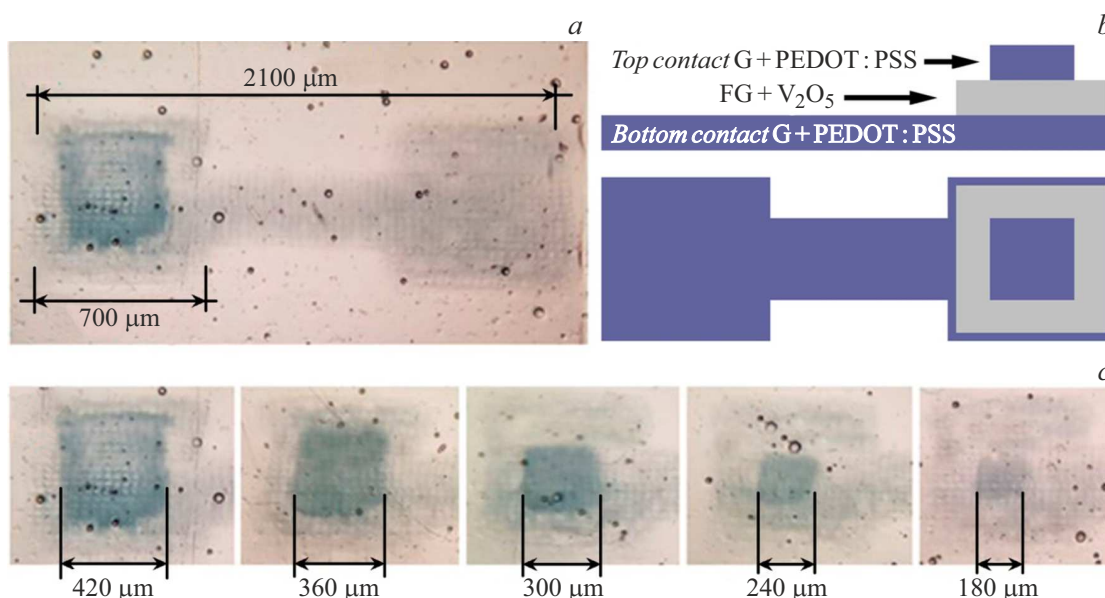


Figure 2. *a* — images of Gr/FG/V₂O₅/Gr structures obtained using an optical microscope; *b* — diagram of the structure of memristors; *c* — bottom row — images of all the upper contacts of structures of different sizes.

roughness is ~ 15 nm in case of printing of the active layer on graphene contacts. Since our structures were printed on PET, and such a substrate has a significantly higher relief, the roughness of such films was not determined in this work.

An array of crossbar structures was printed for the study (Fig. 2). Structures with different upper contact areas were created, which ranged from 180 to 420 μm . A special feature of these structures is the absence of metal contacts that are traditional for memristors. Layers consisting of graphene flakes (Gr) mixed with a conductive polymer PEDOT:PSS (poly(3,4-ethylenedioxythiophene) polystyrene sulfonate) were printed as contacts, which improves the binding of graphene flakes and increases the conductivity of the composite layer. The resistance of the graphene flake film decreases after adding 10⁻³ mass.% PEDOT: PSS

from 4.5 k Ω/\square to 20–50 Ω/\square . It is also worth noting the dependence of conductivity on the number of printed layers. The resistance decreases with an increase of the number of printed layers and at a thickness of ~ 400 nm reaches values of 20–50 Ω/\square .

Fig. 3, *a* shows the results of measurement of the current-voltage characteristics for one of Gr/FG/V₂O₅/Gr structures, where the thickness of the active layer of memristor was 30–40 nm. Bipolar switching is observed with the ratio of currents in the open ON and closed OFF states of ~ 2 orders of magnitude. The switching voltage for these structures is 1.0–1.5 V. The dependence of the open state current for these structures on the upper contact area shows a strong increase in the open state current (Fig. 3, *b*). This indicates the conductivity of the memristor over localized states in this case, the current value increases with the increase of the

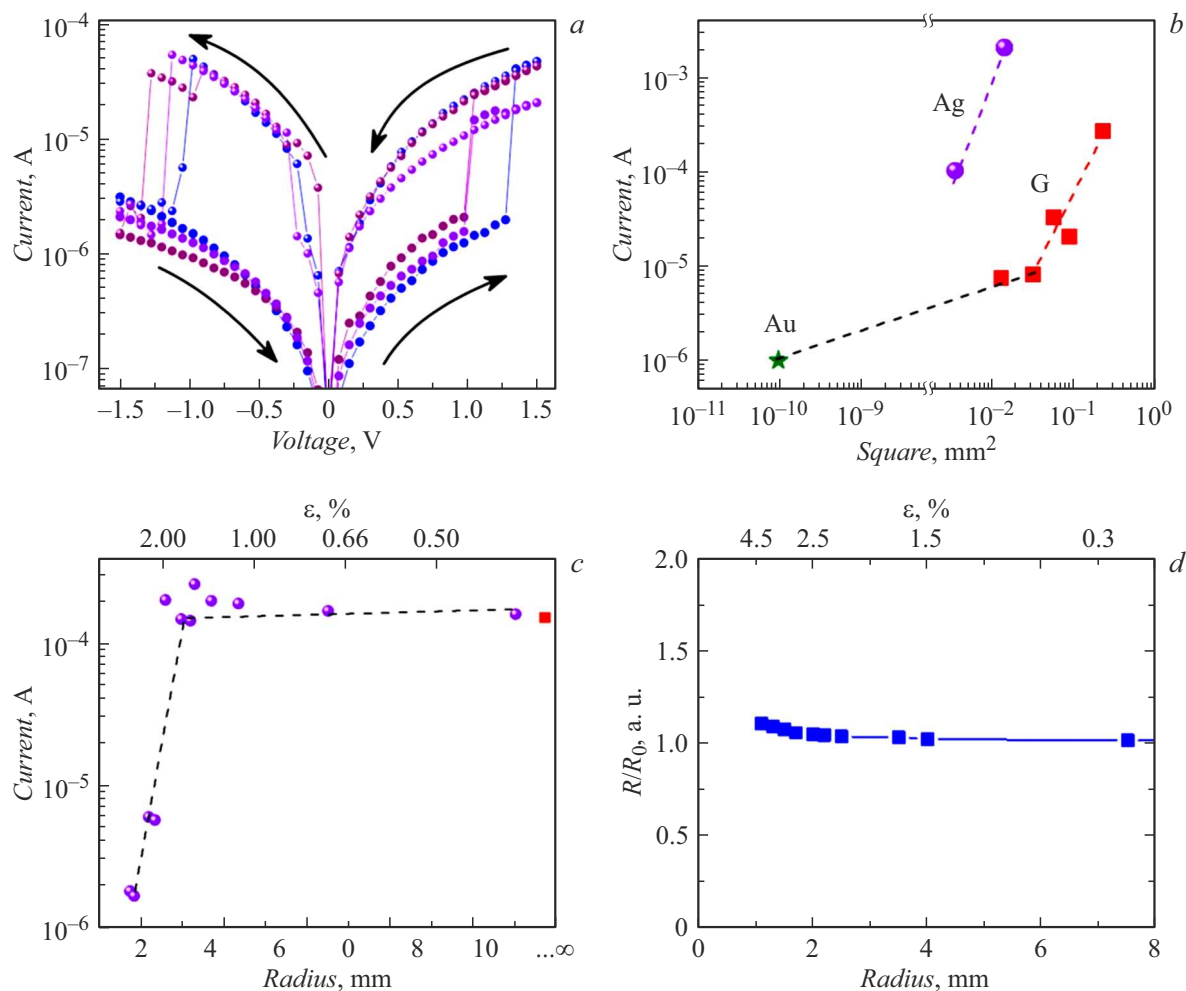


Figure 3. Characteristics of crossbars of memristors with graphene contacts and a thickness of active layer of FG/ V_2O_5 nanoparticles 30–40 nm. *a* — the current-voltage curves of the memristor structure are represented modulo in logarithmic scale for better visualization; *b* — dependence of the open-state current on the area of structures with silver, graphene, and gold contacts, in the latter case, measurements were made using an atomic force microscope probe; *c* — change of the open-state current depending on the bending radius and tensile deformations that occur during structure bending; *d* — change of the resistance of graphene contacts during bending as a result of tensile deformations.

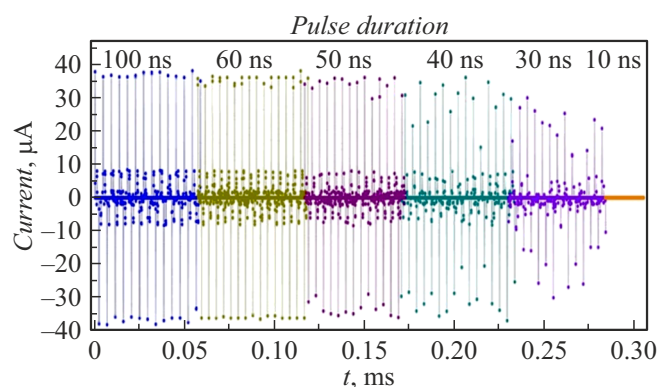


Figure 4. Pulse switching of Gr/FG/ V_2O_5 /Gr structures with varying pulse duration from 10 to 100 ns. Opening pulse voltage was 2.5 V, and the amplitude of the test pulse was 0.5 V.

area of the structure. For comparison, Fig. 3, *b* shows data on the open-state current dependence for similar structures with silver contacts created by 2D-printing. The open-state current values in such memristors are higher than for the Gr/FG/ V_2O_5 /Gr structures, and the functional dependence is similar. The change of the current ON of memristors in case of change of the contact material is a known fact [13], and the functional dependence of the current on the area of the structure reflects the physical processes in the active material of the memristor that occur when it is switched to the open state. It was found that the threshold voltage of memory effect activation is closely related to the electrochemical activity of metals. In particular, if non-inert metals (for example, Ag) are used as electrical contacts, the diffusion of metal atoms into the active layer of the memristor with the formation of metal bridges can contribute to the conductivity in the open state [14]. Fig. 3, *b*

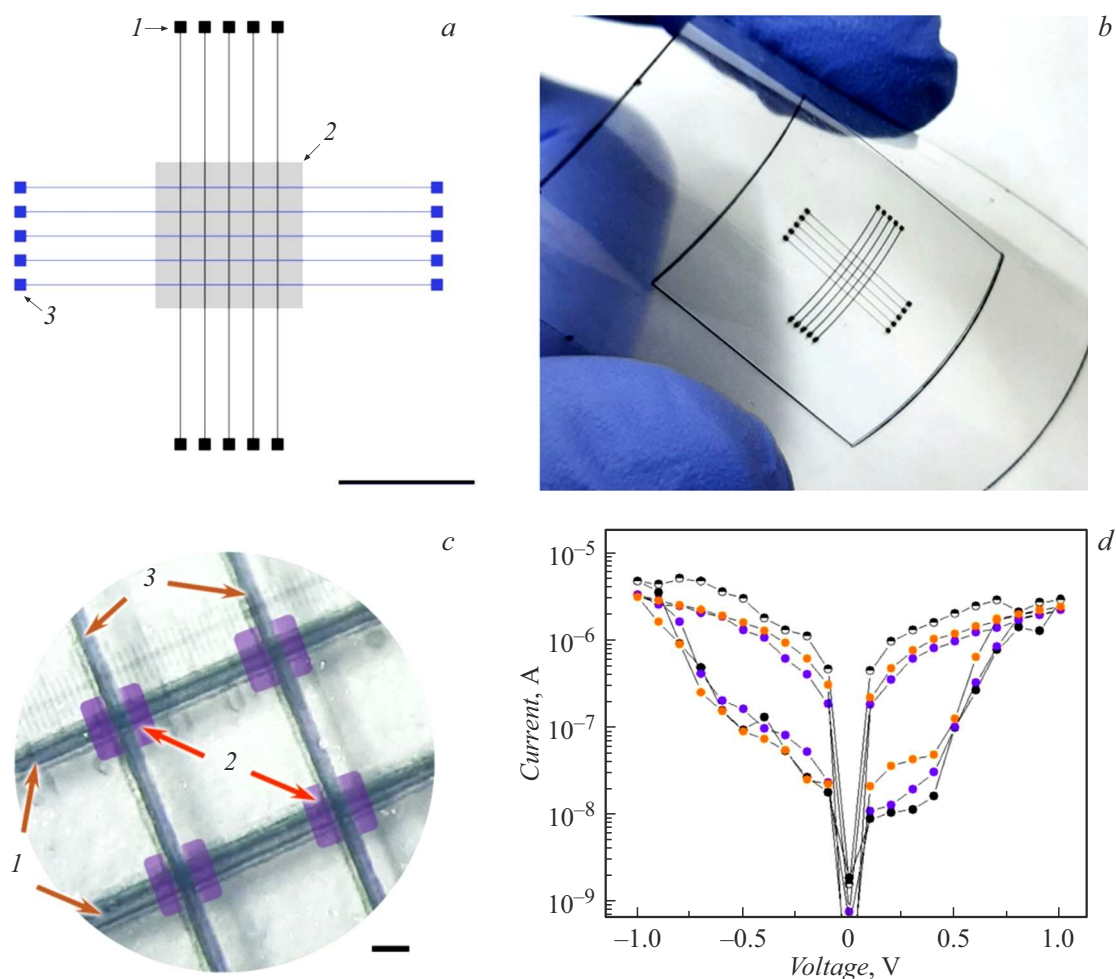


Figure 5. Printed crossbar matrix on a flexible substrate: *a* — schematic image of the printed pattern, numbers indicate the sequence of printed elements of the matrix, the size difference is 0.5 cm; *b* — photo image of the printed structure on a flexible polymer substrate; *c* — photo image of printed crossbar structures. The digits 1 and 3 indicate the lower and upper contacts, respectively, with blue squares and the number 2 indicates the area of application of the memristor material, the size range 100 μm ; *d* — current-voltage curve of the memristor element of the matrix.

shows the value of the open-state current for a cluster of several $\text{FG}/\text{V}_2\text{O}_5$ nanoparticles on gold, measured using a Si/Au probe of an atomic force microscope. This point, due to the use of an inert material, fits into a weaker dependence on the contact area.

The results of measurements during bending of structures are shown in Fig. 3, *c*. The mechanical deformation ε that occurred in the film was estimated using the expression $\varepsilon = (d + t)/2r$ [15], where d is the flexible substrate thickness (100 μm), t is the film thickness, r is the bending radius of the substrate. In this case, the film thickness t can be neglected compared to the substrate thickness. Fig. 3, *c* shows that the structures remain functional and exhibit memristor characteristics without changing the parameters up to 2% deformation (bending radius of ~ 2.5 mm). The current sharply decreases in the open state with the greater deformation, but it is restored to its original value when the mechanical stress is removed. The results obtained indicate that there was no irreversible degradation of the memristor

during bending, i.e. mechanical destruction of structures. With bending of the film, the effective width of potential barriers between particles in the working layer increases, which reduces the conductivity of memristors.

Fig. 4 shows the pulse measurements with opening pulse voltages of 2.5 V and a testing pulse amplitude of 0.5 V. The opening pulse duration varied from 10 to 100 ns in increments of 10 ns. Full-fledged switching was observed starting with the pulse duration of 30 ns. It was shown in [10] for a memristor with an active layer of $\text{FG}/\text{V}_2\text{O}_5$ nanoparticles and silver contacts that the switching time was also ~ 30 ns.

High-quality printed matrices of crossbar structures on flexible PET substrates are manufactured based on the composite material $\text{FG}/\text{V}_2\text{O}_5$. Contacts are printed from a composite material based on graphene particles and PE-DOT:PSS polymer. The diagram of the pattern developed for 2D-printer is shown in Fig. 5, *a*, track width is 50 μm , the size of the contact pads is 300 \times 300 μm . The numbers

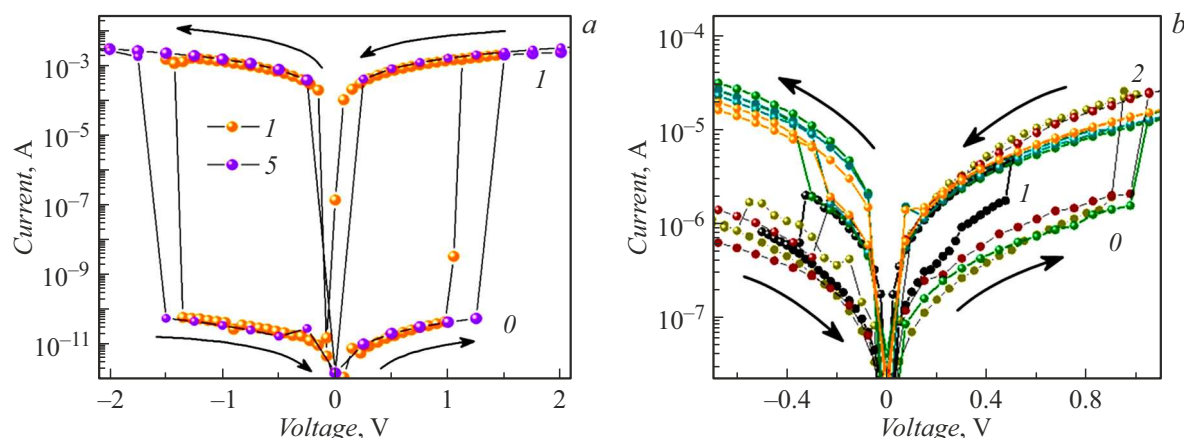


Figure 6. Current-voltage curves of structures with different active layer thickness and structure area of $60 \times 60 \mu\text{m}$. Active layer thickness: *a* — ~ 60 nm (Ag contacts), *1* and *5* — sequence number on (*A*) measured CVC; *b* — $20\text{--}30$ nm (graphene contacts). Digits *0* indicate the closed state, and *1, 2* — open states.

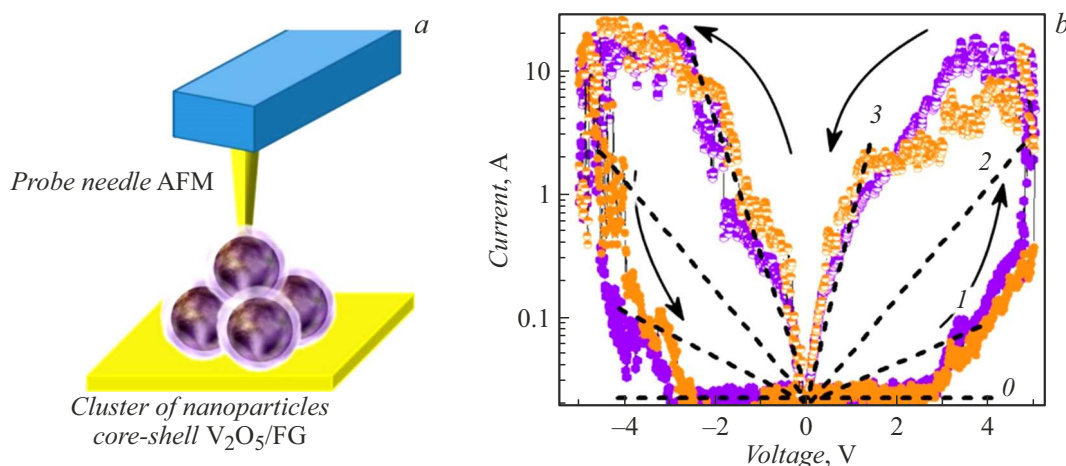


Figure 7. *a* — schematic image of a particle cluster measured using an atomic force microscope probe; *b* — current-voltage curves of structures with an active layer thickness of $10\text{--}15$ nm (two-layer cluster). Digits *0* indicate a closed state, and *1–3* indicate open states.

indicate the sequence of drawing matrix fragments: lower contacts *1*, active memristor layer made of composite material *2*, upper contacts *3*.

Fig. 5, *b, c* shows photo images of the printed matrix and memristor structures of the matrix, respectively. The area of application of the memristor material is indicated by squares and a number *2*. The characteristic current-voltage curves of the printed memristor structure are shown in Fig. 5, *d*. Bipolar resistive switching of up to 2 orders of magnitude is observed.

Reduction of the thickness of the memristor layer of structures and the contact area results in a change of the current-voltage characteristics. Fig. 6 and 7 show typical current-voltage curves of the Gr/FG/ V_2O_5 /Gr structures for the memristor active layer thicknesses of ~ 60 , $20\text{--}40$, $10\text{--}15$ nm. The contact areas were equal in the first two cases, the latter structures were measured using an AFM probe, and the area of the upper contact can be estimated as $10\text{--}20 \text{ nm}^2$. The current in the closed state increased

with a decrease of the thickness of the memristor layer, the opening voltage decreased, and in some cases a multi-level transition from the closed state to the open state was observed. There are two open states as shown in Fig. 6, *b*. The transition to measurements on clusters of $3\text{--}4$ particles (Fig. 7, *b*, cluster size $\sim 10\text{--}15$ nm) using an atomic force microscope probe showed that for this case the current-voltage curves demonstrate a smooth transition between the open and closed states by an $3\text{--}4$ order of magnitude. Moreover, well-reproducible features of the current-voltage curves, namely small plateaus, allow distinguishing three-level switching. Thus, the transition to nanoparticle clusters makes it possible to form several (in our case, three) permitted states and provides more opportunities for creating multi-level memory with the capability to store more information with the same number of elements. More detailed information about measurements on clusters of $2\text{--}3$ particles is provided in [10].

Thus, the parameters of the Gr/FG/V₂O₅/Gr structures demonstrate the possibility of creation of non-volatile memory, multi-level memory with low power consumption. The switching power of the structure W was estimated using a simple formula, which took into account: the opening voltage V_{ON} , the open-state current I_{ON} and the closed-state current $I_{OFF}W = (I_{ON} - I_{OFF})V_{ON}$. In the result the values of 1.0–1.3 mW for Ag/FG/V₂O₅/Ag structures, 18–30 μ W for Gr/FG/V₂O₅/Gr on the SiO₂/Si substrate, and 1–2 μ W for Gr/FG/V₂O₅/Gr were obtained on a flexible substrate. The time used for switching structures to the open state during pulse measurements was taken into account (100 ns) to estimate the switching energy, and it was found that the switching energy for the same structures was \sim 1 nJ, \sim 100 \sim 1.8 fJ, respectively. When compared with data from various works from [16], the obtained power is the lowest, especially for flexible structures.

The reduction of the lateral dimensions of elements will allow placement of elements vertically, creating different 3D-architectures for devices. By varying the ratio of the thickness of the active layer and the lateral dimensions of elements, it is possible to significantly control the parameters of the resulting memory elements.

Conclusions

The technology for creating and using 2D-printing arrays of Gr/FG/V₂O₅/Gr structures with a working layer of FG-encapsulated V₂O₅ nanoparticles and contact layers of graphene flakes (without the use of metal particles). Switching events of up to two orders of magnitude with switching voltages of 1–1.5 V with an active layer thickness of \sim 20–40 nm were obtained on such memristors. Structures with graphene contacts were studied by subjecting them to tensile deformations which occur at bending. The open state current did not change until the bending radius was 2.5 mm, which corresponds to the deformation \sim 2%, after which the current value decreased. However, after the deformation was removed, the switching parameters returned to the original state. This shows that memristors based on the material FG/V₂O₅ can be used in flexible electronics devices. Reduction of the geometric parameters of structures Gr/FG/V₂O₅/Gr (active layer thickness and structure size) demonstrates the possibility of creating non-volatile and multi-level memory with low energy consumption.

Funding

The fabrication of the memristor was supported by the Ministry of Science and Higher Education of the Russian Federation. The study of the properties of memristors was supported by the Russian Science Foundation (project ID: 22-19-00191).

Conflict of interest

The authors declare that they have no conflict of interest.

References

- [1] J. Zhu, T. Zhang, Y. Yang, R. Huang. *Appl. Phys. Rev.*, **7**, 011312 (2020).
- [2] P. Tufan, K.S. Pranab, M. Soumen, K.K. Chattopadhyay. *ACS Appl. Electron. Mater.*, **2** (11), 3667 (2020).
- [3] D. Ielmini, Z. Wang, Y. Liu. *APL Mater.*, **9**, 050702 (2021).
- [4] Y. Chen. *ReRAM: History, Status, and Future*. *IEEE Trans. Electron. Devices*, **67**, 1420 (2020).
- [5] B. Li, J.R. Doppa, P.P. Pande, K. Chakrabarty, J.X. Qiu, H. Li, *ACM J. Emerg. Technol. Comput. Syst. (JETC)*, **16**, 1 (2020).
- [6] C. Bengel, F. Cüppers, M. Payvand, R. Dittmann, R. Waser, S. Hoffmann-Eifert, S. Menzel. *Front. Neurosci.*, **15**, 661856 (2021).
- [7] A.I. Ivanov, A.K. Gutakovskii, I.A. Kotin, R.A. Soots, I.V. Antonova. *Adv. Electron. Mater.*, **5** (10), 1900310 (2019).
- [8] W.K. Kim, C. Wu, T.W. Kim. *Appl. Surf. Sci.*, **444**, 65 (2018).
- [9] R. Ge, X. Wu, M. Kim, J. Shi, S. Sonde, L. Tao, Y. Zhang, J.C. Lee, D. Akinwande. *Nano Lett.*, **18**, 434 (2018).
- [10] A.I. Ivanov, V.Ya. Prinz, I.V. Antonova, A.K. Gutakovskii. *Phys. Chem. Chem. Phys.*, **23**, 20434 (2021).
- [11] I.V. Antonova, I.I. Kurkina, A.K. Gutakovskii, I.A. Kotin, A.I. Ivanov, N.A. Nebogatikova, R.A. Soots, S.A. Smagulova. *Mater. Des.*, **164**, 107526 (2019).
- [12] O. Berezina, D. Kirienko, A. Pergament, G. Stefanovich, A. Velichko, V. Zlomanov. *Thin Solid Films*, **574**, 15 (2015).
- [13] J.C. Pérez-Martínez, M. Berruet, C. Gonzales, S. Salehpour, A. Bahari, B. Arredondo, A. Guerrero. *Adv. Funct. Mater.*, **33**, 2305211 (2023).
- [14] V. Aglieri, A. Zaffora, G. Lullo, M. Santamaria, F.Di Franco, U.Lo Cicero, M. Mosca, R. Macaluso. *Superlat. Microstruct.*, **113**, 135 (2018).
- [15] J. Zhao, C. He, R. Yang, Z. Shi, M. Cheng, W. Yang, G. Xie, D. Wang, D. Shi, G. Zhang. *Appl. Phys. Lett.*, **101** (6), 063112 (2012).
- [16] J.-L. Meng, T.Y. Wang, Z. Yu He, L. Chen, H. Zhu, L. Ji, Q.Q. Sun, S.-J. Ding, W.-Z. Bao, P. Zhou, D.W. Zhang. *Mater. Horizons*, **8**, 538 (2021).

Translated by A.Akhtyamov